Available online at www.sciencedirect.com

ScienceDirect

Procedia Engineering10 (2011) 415–420

Engineering Procedia

ICM11

Identification of GTN model parameters by application of response surface methodology

M. Abbasi[a], M. Ketabchi[a], H. Izadkhah[a], D. H. Fatmehsaria[a], A. N. Aghbash[b], a*

[a]*Amirkabir University of Technology, 424 Hafez Ave., Tehran, Iran*
[b]*Shahid BeheshtiUniversity, Evin, Tehran, Iran*

Abstract

A reliable prediction of ductile failure in metals is still a wide-open matter of research. Among different models, Gurson-Tvergaard-Needleman (GTN) has been used extensively. One major issue is the accurate identification of GTN model parameters, which it is not possible to perform experiments for their evaluation. In the present paper a novel inverse procedure aimed to estimate the material parameters of the GTN porosity-based plastic damage model by means of RSM method is represented. The results showed good agreement between experimental and predicted forming limit diagrams when determined GTN parameters were utilized. FE-simulation by means of Abaqus software used to predict FLDs.

Selection and peer-review under responsibility of ICM11

Keywords: GTN model ; Forming limit diagram; Response surface methodology; Simulation.

1. Introduction

A Forming Limit Diagram (FLD) is a graph which depicts the major strains (ε_1) for all values of the minor strain (ε_2) at the onset of localized necking. Experimental determination of a FLD is usually very time consuming and requires special equipments. Many researchers [1-2] have developed analytical and numerical models as an alternative approaches for coping with these difficulties.

As a matter of engineering knowledge, Gurson-Tvergaard-Needleman (GTN) approach is one of the well known mesomechanical models for ductile fracture [3]. Brunet et al. [4] have successfully applied Gurson-Tvergaard-Needleman (GTN) model to determine the FLDs of Ni-based sheet metal and an

* Corresponding author. Tel.: +98-21-64542949; fax: +98-21-66405846.
E-mail address: m.abbasi@aut.ac.ir .

Selection and peer-review under responsibility of ICM11 doi:10.1016/j.proeng.2011.04.070

aluminium alloy. A literature survey, however, shows that the correct identification of the GTN model parameters is a prerequisite for successful analysis of the ductile failure through GTN damage model [5]. Brunet et al. [6] investigated the FLDs of three aluminium sheets together with a mild-steel sheet employing GTN model. Assuming the Tvergaard coefficients being fixed, the model parameters were adjusted applying a uniaxial tensile test. In their work, the effective parameters were studied by the use of inverse method proposed by Fratini et al. [7].

The identification of pertinent factors for GTN damage model should be carried out employing a suitable design of experiments strategy. Response surface methodology (RSM) is able to simultaneously consider several factors at different levels, and give a second order polynomial model for the relationship between the various factors and the response through the use of central composite design (CCD) [8]. In the present work, GTN damage model parameters are identified through inverse method for an interstitial free (IF) steel, employing response surface methodology. In this regard different sets of GTN model parameters values are selected and a simulation of tensile test is run for each set of values. To compare simulated stress-strain diagram to experimental one, four responses namely as strain at maximum stress (R_1), maximum stress (R_2), strain at failure (R_3) and stress at failure (R_4) are selected as the indicators. Finally, the proposed models based on RSM are optimized by simultaneous mathematical solution. The identified GTN model parameters are defined as input data for ABAQUS software and FLD of studied steel is predicted.

1.1. GTN model

According to Gurson-Tvergaard-Needleman model, local damage is due to nucleation, growth and subsequent coalescence of voids inside the material; these three mechanisms result in a resistance loss which in turn, progressively leads to the failure. Here, the yield potential as an extension of the Gurson–Tvergaard model used in the context of plane-stress for orthotropic materials [9] is represented:

$$\Phi = \frac{q^2}{\sigma_y^2} + 2q_1 f^* \cosh\left(\frac{-3q_2 p}{2\sigma_y}\right) - (1 + q_3 f^{*2}) = 0 \quad (1)$$

where $f^*(f)$ is the damage function of the microvoid volume fraction or porosity (f). Tvergaard considered the constants as q_1=1.5, q_2=1 and $q_3=q_1^2$ for the void volume fraction and pressure terms. q is the effective stress of the macroscopic Cauchy stress tensor and σ_y describes the hardening of a fully dense matrix material. The damage model takes into account three main phases of the damage evolution including nucleation, growth and coalescence [9]:

$$df = df_N + df_G + df_C \quad (2)$$

The nucleation of microvoids is expressed by [4]:

$$df_N = \left(\frac{f_N}{S_N\sqrt{2\pi}}\right) \exp\left\{-\frac{(\bar{\varepsilon}^p - \varepsilon_N)^2}{2S_N^2}\right\} d\bar{\varepsilon}^p \quad (3)$$

The normal distribution of the nucleation strain has a standard deviation of S_N, mean value of ε_N and nucleates voids with a volume fraction of f_N. Growth of the present voids is based on the apparent volume change and the law of mass conservation and is expressed as [4]:

$$df_G = (1-f).(d\varepsilon_{11}^p + d\varepsilon_{22}^p + d\varepsilon_{33}^p) \quad (4)$$

Finally, regarding the coalescence and final material failure, the modification of the yield condition is introduced through the function $f^*(f)$ specified by Tvergaard [6]:

$$\begin{cases} f^* = f & f < f_c \\ f^* = f_c + \delta(f - f_c) & f \geq f_c \end{cases} \quad (5)$$

With:

$$\delta = \frac{(f_u^* - f_c)}{(f_f - f_c)} \qquad f_u^* = \frac{1}{q_1}$$

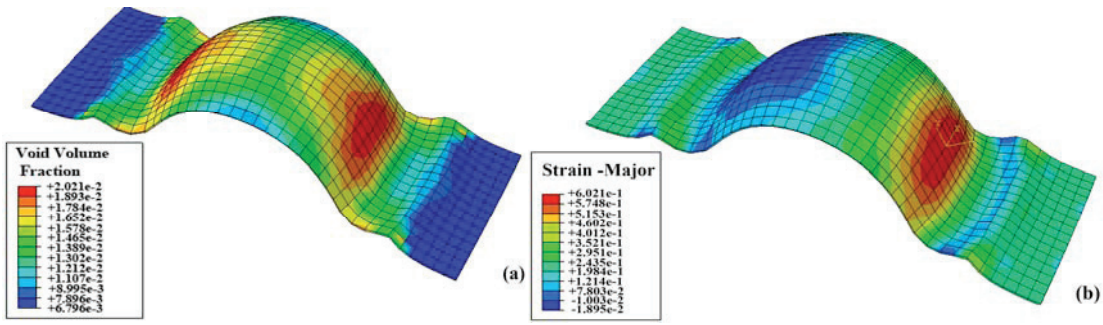

Fig. 1 Simulation results for blank with 75 mm width and when f=f_f, (a) void volume fraction; (b) major surface strain.

f_u^* is the ultimate value of f^* at ductile rupture. f_c is the critical void volume fraction when the coalescence of microvoids occurs and the load bearing capability of the material sharply drops. Finally, f_f is the void volume fraction when the stress-capability completely vanishes (final failure). As it comes from the reminded relations, identification of GTN model parameters (f_0, f_c , f_R , ε_N , S_N , f_N) is essential in order to analyze tearing of ductile materials.

2. Material and methods

2.1. Material

IF-steel, due to its high ductility and formability, was selected as the sample test. Table 1 lists the mechanical properties of studied IF-steel, which are obtained through tensile test based on ASTM-E8 Standard [10].

Table 1 Mechanical properties and thickness of studied steel.

Y.S (*MPa*)	U.T.S (*MPa*)	Elongation (*%*)	n	K (*MPa*)	Thickness (*mm*)
160	280	48.5	0.23	435	1.1

2.2. Tensile Test

Among six major GTN damage model parameters- initial void volume fraction (f_0), effective void volume fraction (f_N), critical void volume fraction (f_c), final void volume fraction (f_f), mean (ε_N) and standard deviation (S_N) of the normal distribution of the nucleation strain- the last two ones were assumed to be constant ($\varepsilon_N = 0.1$, $S_N = 0.1$) [11]. The procedure followed to obtain domain change of other factors is explained carefully in Ref. [12]. A central composite design (CCD) was adopted to study the other four factors at three levels and correspondingly different sets of parameters values were achieved. Each set of values were defined as the input data for ABAQUS and the tensile test was simulated. Simulation of tensile test was carried out by Abaqus/Explicit. It was assumed that the material is isotropic with elastic-plastic behaviour which obeys a power-law hardening rule. Modelled parts were discretized by C3D8R elements. In the simulations, element sizes of 3 mm with one layer of through thickness elements were used.

2.2. FLD test

Hecker method [13] was utilized for determining the experimental FLD. Circle-grid pattern with a diameter of 2.5 mm were used to measure surface strains. Simulation of Hecker test was carried out applying ABAQUS software. An elastic-plastic characteristic was defined for the blank which obeyed porous metals plasticity. Identified GTN model parameters were defined for software and thereby the forming process was simulated. For each specimen, major and minor surface strains of the element in which $f=f_f$, were selected as the failure strains. In Fig. 1a and Fig. 1b for a blank with 75 mm width, respectively the void volume fractions of different elements and correspondent major surface strain, when critical condition ($f=f_f$) is satisfied, are illustrated. After determination of major and minor failure strains of different specimens, FLD of studied steel was predicted.

2.3. Experimental design for RSM

A central composite design (CCD) was adopted to study four factors at three levels. Twenty eight simulation tensile tests runs were generated with 4 factors and 3 levels by the principle of RSM using MINITAB Release 15. The levels employed for the different factors, according to CCD design as well as correspondent responses obtained from each run, are listed in Table 2. The quadratic polynomial regression model was chosen for predicting the response variable in terms of the four independent variables.

Table 2 Central composite design arrangement and responses.

Experiment Number	Factors				Responses			
	f_0	f_N	f_C	f_f	R_1	R_2	R_3	R_4
1	0.0002	0.001	0.0050	0.050	0.46	431.83	1.11	373.56
2	0.0020	0.001	0.0050	0.050	0.49	426.82	0.49	426.80
3	0.0002	0.045	0.0050	0.050	0.046	221.71	0.046	221.70
4	0.0020	0.045	0.0050	0.050	0.039	211.76	0.055	173.00
5	0.0002	0.001	0.0500	0.050	0.51	431.51	1.36	417.70
6	0.0020	0.001	0.0500	0.050	0.45	429.36	1.28	402.70
7	0.0002	0.045	0.0500	0.050	0.35	369.70	0.35	369.70
8	0.0020	0.045	0.0500	0.050	0.19	300.35	0.18	300.35
9	0.0002	0.001	0.0050	0.200	0.51	431.51	1.14	411.00
10	0.0020	0.001	0.0050	0.200	0.45	429.36	0.82	402.30
11	0.0002	0.045	0.0050	0.200	0.104	238.56	0.18	215.00
12	0.0020	0.045	0.0050	0.200	0.30	320.74	0.36	283.00
13	0.0002	0.001	0.0500	0.200	0.45	431.66	1.46	419.00
14	0.0020	0.001	0.0500	0.200	0.49	429.09	1.23	409.60
15	0.0002	0.045	0.0500	0.200	0.31	330.20	0.37	316.00
16	0.0020	0.045	0.0500	0.200	0.28	320.26	0.40	302.60
17	0.0002	0.023	0.0275	0.125	0.41	391.29	0.52	285.00
18	0.0020	0.023	0.0275	0.125	0.35	369.16	0.46	290.00
19	0.0011	0.001	0.0275	0.125	0.46	430.61	1.43	405.00
20	0.0011	0.045	0.0275	0.125	0.19	316.42	0.26	240.00
21	0.0011	0.023	0.0050	0.125	0.18	301.20	0.24	270.00
22	0.0011	0.023	0.0500	0.125	0.44	407.74	0.77	335.00
23	0.0011	0.023	0.0275	0.050	0.33	371.72	0.33	370.00
24	0.0011	0.023	0.0275	0.200	0.43	394.16	0.62	300.00
25	0.0011	0.023	0.0275	0.125	0.38	374.75	0.49	275.00
26	0.0011	0.023	0.0275	0.125	0.39	375.00	0.49	275.50
27	0.0011	0.023	0.0275	0.125	0.42	406.00	0.52	360.00
28	0.0011	0.023	0.0275	0.125	0.40	377.92	0.47	330.00

Table 3 ANOVA table of the responses

	df				SS				MS				P-values			
	R_1	R_2	R_3	R_4	R_1	R_2	R_3	R_4	R_1	R_2	R_3	R_4	R_1	R_2	R_3	R_4
Total	27	27	27	27	0.54	122519	4.98	142584								
Regression	14	14	14	14	0.43	116026	4.85	129868	0.035	8287.5	0.35	9276.3	0.00	0.00	0.00	0.00
Residual error	13	13	13	13	0.04	6493	0.13	12716	0.003	499.5	0.01	978.2				
Lack of fit	10	10	10	10	0.04	5807	0.12	7401	0.004	580.7	0.013	740.1	0.17	0.42	0.2	0.9
Pure error	3	3	3	3	0.007	686	0.001	5315	0.0002	228.7	0.001	1771.7				
R^2 (%)	92.0	94.7	97.4	91.0												

(df = degrees of freedom; SS = sum of squares; MS = mean squares.)

3. Results and discussion

3.1. Model fitting

Table 2 lists the values of four responses (R_1, R_2, R_3 and R_4) at each of the 28 combination of factor levels. The results of the ANOVA are presented in Table 3; the low p values for the regression ($P<0.01$) and the fact that the lack of fit of the model was not significant ($P>0.1$) indicates the suitability of the model. The values of the regression coefficients were obtained (See Ref. [12]). Both f_N and f_c linear terms and interactive $f_N f_c$ term were significant in the case of R_1, R_2 and R_3; while for R_4, linear f_N and f_f terms together with f_f quadratic term were significant. Additionally, f_0 was statistically insignificant in all responses. Based on the regression coefficients calculated for the responses, polynomial regression model equations- those fitted higher than 90% of the variations in the data- were proposed as follows:

$$\mathbf{R_1} = 0.47 - 4.05\,\mathbf{f_N} + 0.42\,\mathbf{f_c} - 93.08\,\mathbf{f_N^2} + 62.63\,\mathbf{f_N}\,\mathbf{f_c} \quad (6)$$

$$\mathbf{R_2} = 414.6 - 4207.3\,\mathbf{f_N} + 2875.3\,\mathbf{f_c} - 49358.7\,\mathbf{f_c^2} + 33475.6\,\mathbf{f_N}\,\mathbf{f_c} \quad (7)$$

$$\mathbf{R_3} = 0.85 - 33.14\,\mathbf{f_N} + 11.47\,\mathbf{f_c} + 383.2\,\mathbf{f_N^2} - 178.03\,\mathbf{f_N}\,\mathbf{f_c} \quad (8)$$

$$\mathbf{R_4} = 476.4 - 3440.3\,\mathbf{f_N} - 1457\,\mathbf{f_f} + 5848.4\,\mathbf{f_f^2} \quad (9)$$

3.2. Optimization of GTN damage model parameters

Using the proposed second order polynomial equations (Eqs. 1–4), the optimum parameters employing genetic algorithm were determined $f_0 = 0.0002$, $f_N = 0.0106$, $f_c = 0.0134$, $f_f = 0.0216$. More about utilization of genetic algorithm to find optimum values of GTN model parameters can be found in Ref. [12]. To confirm the applicability of the models, confirmation runs using the above–mentioned levels of the parameters were carried out.

3.3. Comparison between experimental and predicted FLD

In Fig. 2 the forming limit curve (curve EXP-FLD) obtained from experiments and separates fracture zone from the other zones is shown. The region above the experimental curve (Exp-FLD) is considered to be un-safe for any particular deformation mode and fracture definitely happens; however for strain combinations under the curve, the potential of tearing is low. Since necking is a subjective process and depends on the measuring accuracy of the equipments as well as skills of the experimenter, occasionally, curve 10% below the FLD related to fracture is plotted and used as a safe FLD curve [13-14]. This curve (Exp-FLD- 10% below) has been illustrated in Fig. 2. In Fig. 2 the constructed forming limit curve together with the predicted FLD are depicted. As observed in Fig. 2, predicted FLD shows good compatibility to the experimental safe FLD.

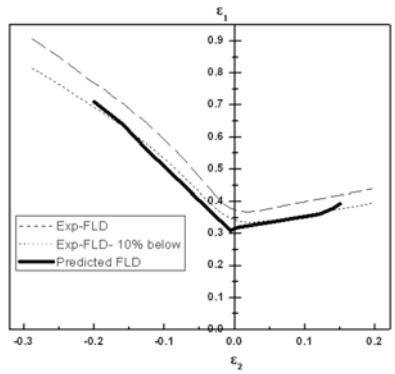

Fig. 2 Comparison among different FLDs obtained via experiments and prediction.

4. Conclusions

In the present work, GTN damage model parameters were identified through inverse method for an IF-steel employing RSM – CCD. By the use of optimized levels of the factors based on RSM – CCD, the predicted FLD was in good agreement with experimental one. As appropriate identification of GTN damage model parameters has brought the possibility of proper analysis of formability, the application of statistical methodology is recommended for evaluation and identification of the correct values of the GTN model parameters.

References

[1] Ahmadi S, Eivani AR, Akbarzadeh A. An experimental and theoretical study on the prediction of forming limit diagrams using new BBC yield criteria and M-K analysis. Comp Mater Sci 2008; **44**: 1272-1280.

[2] Aghaie-khafri M, Mahmudi R, Pishbin H. Role of yield criteria and hardening laws in the prediction of forming limit diagrams. Metall Mater Trans A 2002; **33**: 1363-1371.

[3] Zhiying C, Xianghuai D. The GTN damage model based on Hill'48 anisotropic yield criterion and its application in sheet metal forming. Comp Mater Sci 2009; **44**: 1013-1021.

[4] Brunet M, Morestin F, Walter H. Damage identification for anisotropic sheet-metals using a non-local damage model. Int J Damage Mech 2004; **13**: 35-57.

[5] Sprinmnann M, Kuna M. Determination of ductile damage parameters by local deformation fields: measurement and simulation. Arch Appl Mech 2006; **75**: 775-797.

[6] Brunet M, Mguil S, Morestin F. Analytical and experimental studies of necking in sheet metal forming processes. J Mater Proc Technol 1998; **80-81**: 40-46.

[7] Fratini L, Lombardo A, Micari F. Material characterization for the prediction of ductile fracture occurrence: an inverse approach. J Mater Proc Technol 1996; **60**: 311–316.

[8] Montgomery DC. *Design and analysis of experiments*. New York: John Wiley & Sons; 2006.

[9] Thomason PF. *Ductile fracture of metals*. London: Pergamon Press; 1990.

[10] ASTM Standards. Standard test methods for tension testing of metallic materials. ASTM E8-E8M; 2009.

[11] Abaqus/6.9 Software, Abaqus Analysis User's Manual (6.9), Porous metal plasticity; 2009.

[12] Abbasi M. Analysis of wrinkling and tearing of tailor welded blank during deep drawing process, Ph. D. Thesis, Amirkabir University of Technology, Tehran, Iran; 2011.

[13] Ozturk F, Lee D. Experimental and numerical analysis of out-of-plane formability test. J Mater Proc Technol 2005; **170**: 247-253.

[14] Hosford WF, Caddell RM. *Metal forming-mechanics and metallurgy*. Cambridge: Cambridge University Press; 2007.